Ammonia and temperature sensing applications using fluorometric and colorimetric microparticles and polymeric films doped with BODIPY-emitters

Bertolo, E., Beatriz S. Cugnasca, Frederico Duarte, Hugo M. Santos, José Luis Capelo-Martínez, Alcindo A. Dos Santos and Carlos Lodeiro

Ammonia and Temperature Sensing applications using Fluorometric and Colorimetric micro particles and polymeric films doped with BODIPY-emitters

Beatriz S. Cugnasca[a,b], Frederico Duarte[b], Hugo M. Santos[b], José Luis Capelo-Martinez[b,c], Emilia Bertolo[d], Alcindo A. Dos Santos [a]* and Carlos Lodeiro[b,c,d]**

[a]*Institute of Chemistry, Department of Fundamental Chemistry, University of São Paulo, 05508-000 São Paulo, SP, Brazil*
[b]*BIOSCOPE Research Group, LAQV-REQUIMTE, Department of Chemistry, NOVA School of Science and Technology, FCT NOVA, NOVA University Lisbon, 2829-516 Caparica, Portugal*
[c]*PROTEOMASS Scientific Society, 2825-466 Costa da Caparica, Portugal*
[d] *Section of Natural and Applied Sciences, School of Psychology and Life Sciences, Canterbury Christ Church University, CT1 1QU Canterbury, United Kingdom.*

Corresponding authors: *alcindo@iq.usp.br and **cle@fct.unl.pt

Summary

1. Photophysical characterization of BODIPYs

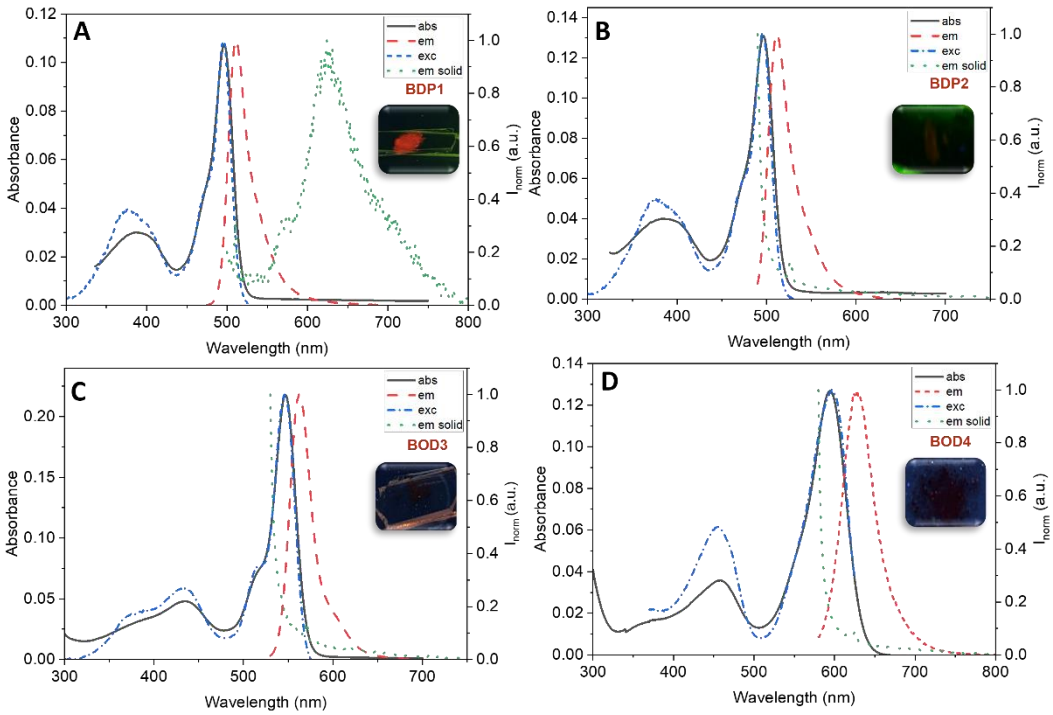

Fig. S1. Absorption, normalized excitation and emission (in solution and in the solid state) spectra of compounds **A) BDP1**, **B) BDP2**, **C) BDP3**, and **D) BDP4** in THF. Conditions: T = 298 K; [BODIPY] = 2 µmol/L. **BDP1** (λ_{ex} = 465 nm, λ_{em} = 540 nm, slit 2.5 nm), **BDP2** (λ_{ex} = 480 nm, λ_{em} = 540 nm, slit 2.5 nm), **BDP3** (λ_{ex} = 520 nm, λ_{em} = 585 nm, slit 2.5 nm), **BDP4** (λ_{ex} = 570 nm, slit 5.0 nm; λ_{em} = 635 nm, slit 10.0 nm).

2. Studies with BODIPY-doped Polymer films

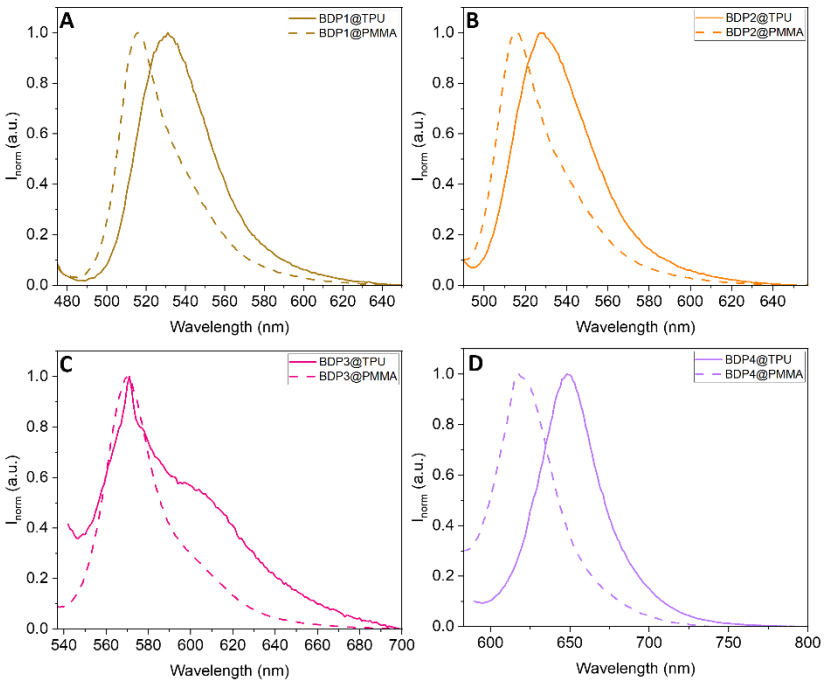

Fig. S2. Normalized emission spectra of polymer doped with BODIPYs in PMMA and TPU matrix. **A) BDP1** (λ_{ex} = 465 nm, slit 1.0); **B) BDP2** (λ_{ex} = 480 nm, slit 1.0; **C) BDP3** (λ_{ex} = 520 nm, slit 2.0); **D) BDP4** (λ_{ex} = 570 nm, slit 2.5).

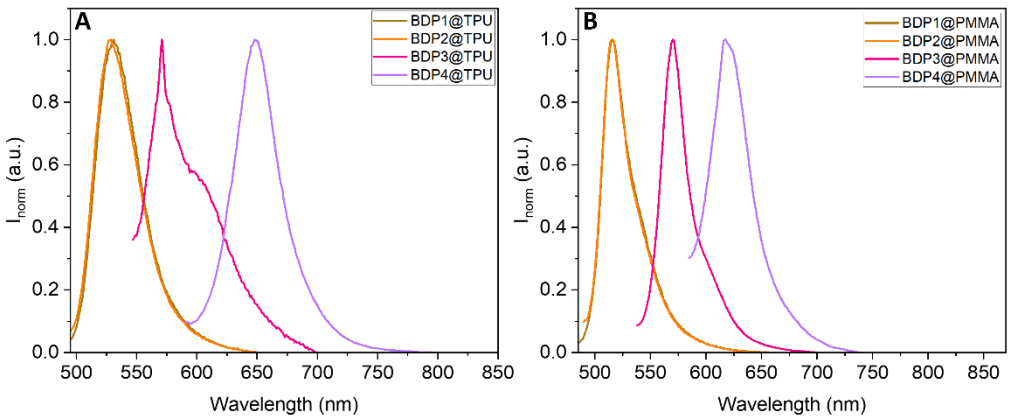

Fig. S3. Normalized emission spectra of polymer doped with BODIPYs in **A)** TPU matrix and **B)** PMMA matrix. Conditions: **BDP1** (λ_{ex} = 465 nm, slit 1.0); **BDP2** (λ_{ex} = 480 nm, slit 1.0; **BDP3** (λ_{ex} = 520 nm, slit 2.0); **BDP4** (λ_{ex} = 570 nm, slit 2.5).

a. Heating and cooling cycles with BODIPY-doped Polymer films

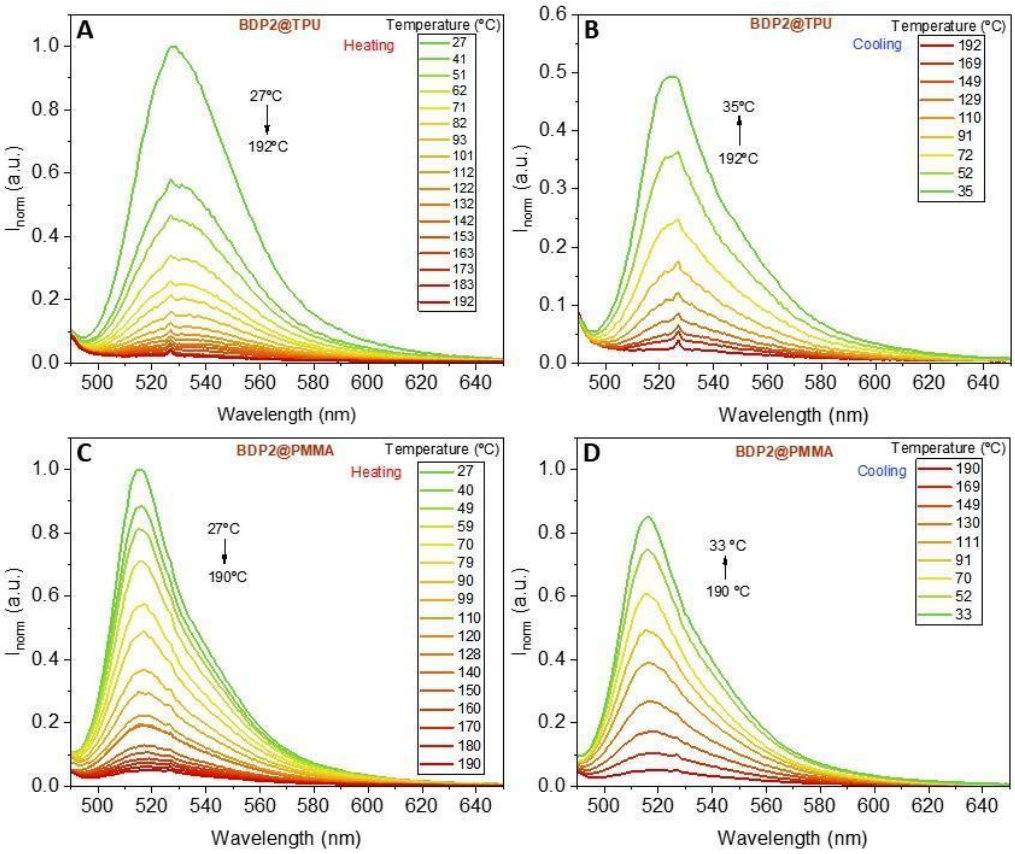

Fig. S4 Emission spectra of **BDP2@TPU** under **A)** heating (27ºC to 192ºC) and **B)** cooling (192ºC to 35ºC) obtained in different temperatures. Emission spectra of **BDP2@PMMA** under **C)** heating (27ºC to 190ºC) and **D)** cooling (190ºC to 33ºC) obtained at different temperatures. λ_{ex} = 480 nm, slit 1.0 nm.

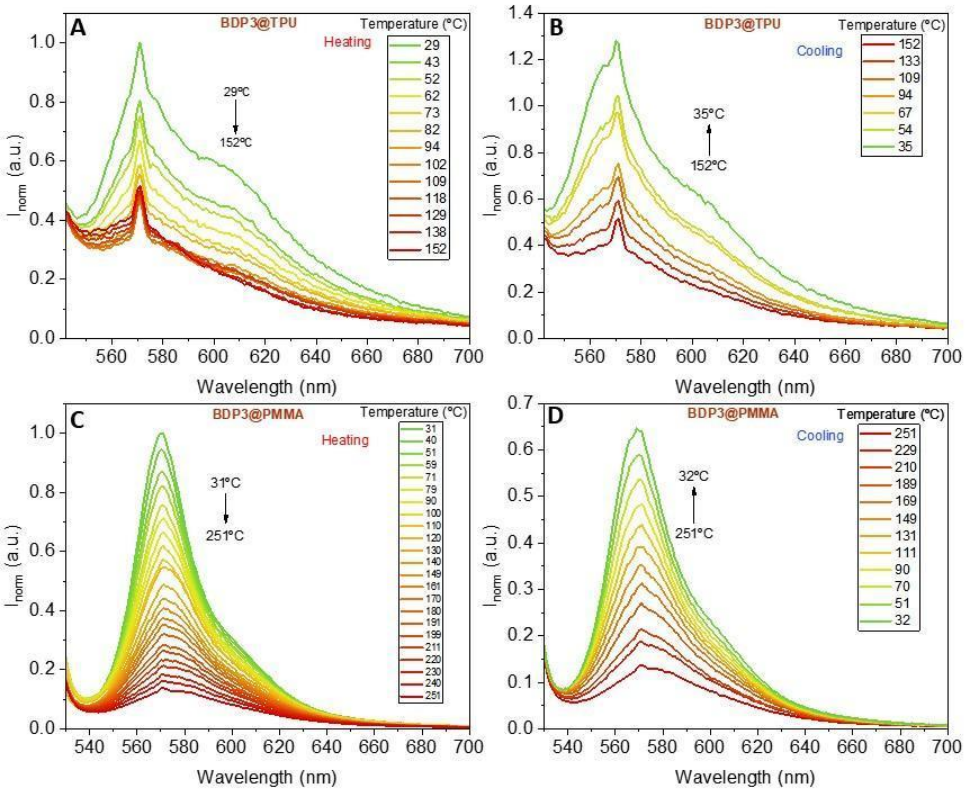

Fig. S5 Emission spectra of **BDP3@TPU** under **A)** heating (29 ºC to 152 ºC) and **B)** cooling (152 ºC to 35 ºC) obtained at different temperatures. Emission spectra of **BDP3@PMMA** under **C)** heating (31 ºC to 251 ºC) and **D)** cooling (251 ºC to 32 ºC) obtained at different temperatures. λ_{ex} = 520 nm, slit 2.0 nm.

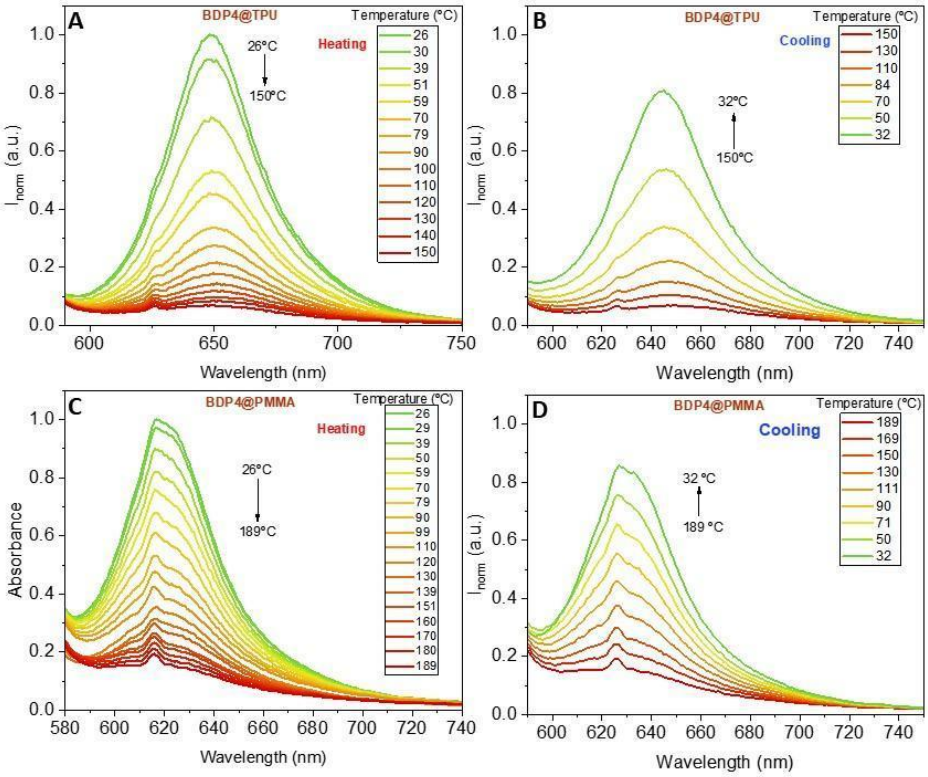

Fig. S6 Emission spectra of **BDP4@TPU** under **A)** heating (26 ºC to 150 ºC) and **B)** cooling (150 ºC to 32 ºC) obtained in different temperatures. λ_{ex} = 570 nm, slit 2.5 nm Emission spectra of **BDP4@PMMA** under

C) heating (26 ºC to 189 ºC) and **D)** cooling (189 ºC to 32 ºC) obtained at different temperatures. λ_{ex} = 570 nm, slit 3.0 nm

Table S1. Emission intensity recovery (%) after heating / cooling cycles of polymer films

Polymer	%recovery	Polymer	%recovery
BDP1-PMMA	74	**BDP1-TPU**	57
BDP2-PMMA	85	**BDP2-TPU**	50
BDP4-PMMA	85	**BDP4TPU**	81

b. Studies of the reaction between BODIPY-doped Polymer films and NH_4OH

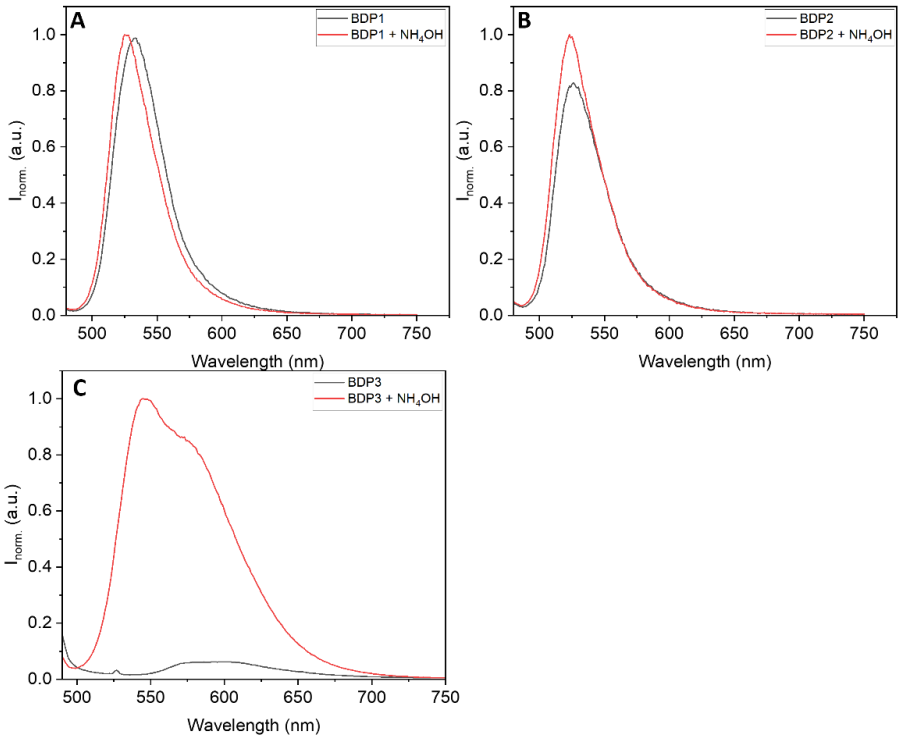

Fig. S7. Emission spectra of polymer doped with BODIPYs in TPU matrix after 1 hour reaction with NH_4OH (5 mol/L). Conditions: **BDP1:** λ_{ex} = 465 nm, slit 1.0 nm; **BDP2:** λ_{ex} = 465 nm, slit 1.0 nm; **BDP3:** λ_{ex} = 480 nm, slit 2.0 nm.

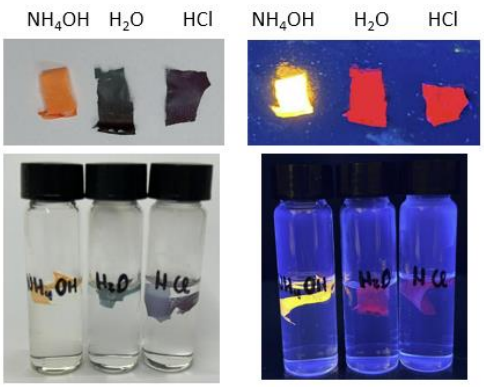

Fig. S8. Above: images of **BDP4@TPU** after reaction with NH_4OH (5 mol/L) and HCl (5 mol/L) for 100 min, under visible light and UV light. Control experiment uses MilliQ water. Below: **BDP4@TPU** dipped into solutions of NH_4OH (5 mol/L), HCl (5 mol/L) and water.

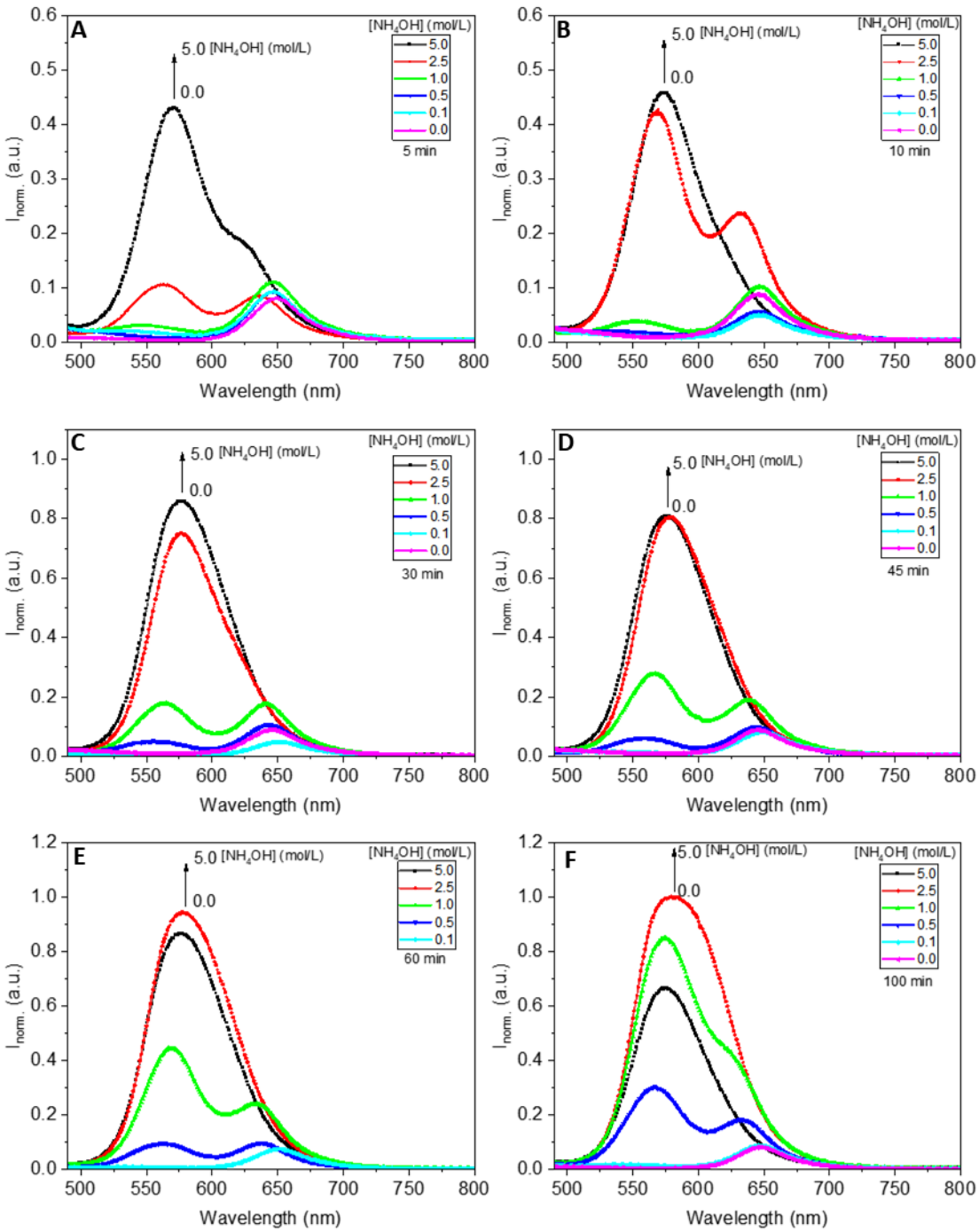

Fig. S9 Emission spectra of **BDP4@TPU** after dipping the polymer in solutions containing different concentrations of NH_4OH (0 – 5 mol/L) after **A)** 5 min, **B)** 10 min, **C)** 30 min, **D)** 45 min, **E)** 60 min, **F)** 100 min reaction. λ_{ex} = 440 nm, slit 2.0 nm. Obs: Spectra normalized with respect to maximum emission in NH_4OH 2.5 mol/L after 100 min of reaction.

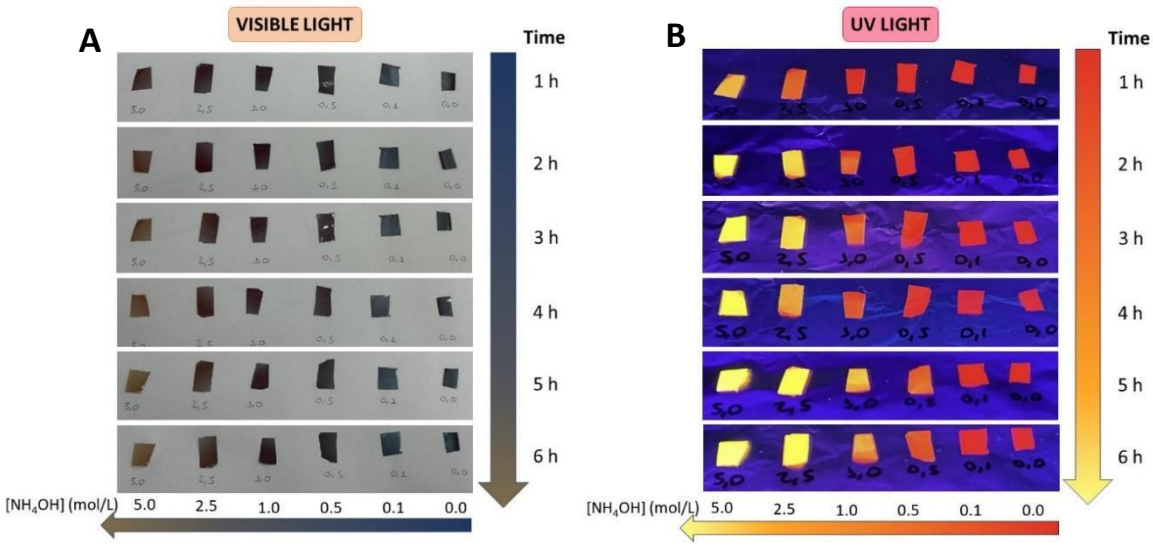

Fig. S10. Images of **BDP4@PMMA A)** under visible light and **B)** under UV light after reaction with different concentrations of NH_4OH (0 – 5 mol/L) and reaction times (10 – 100 min).

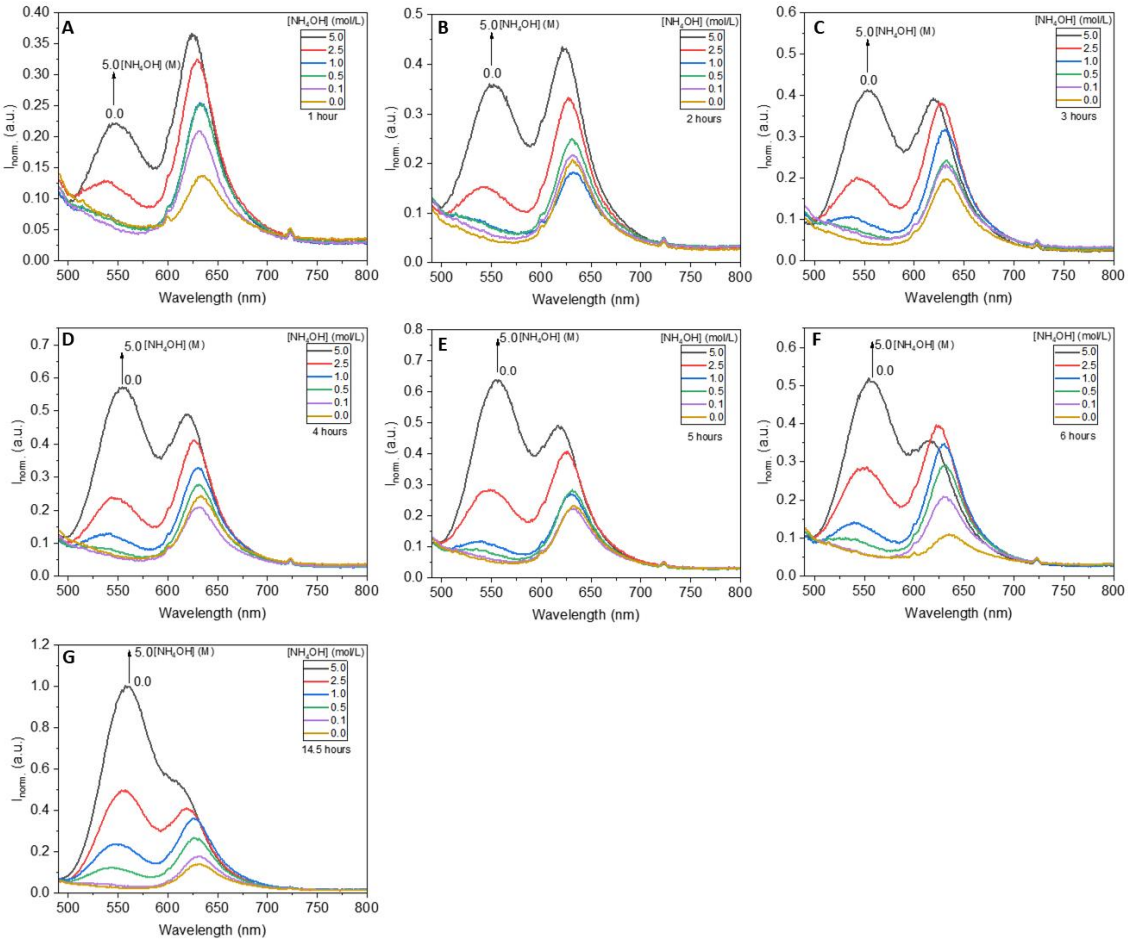

Fig. S11. Emission spectra of **BDP4@PMMA** after dipping the polymer in solutions containing different concentrations of NH_4OH (0 – 5 mol/L) after **A)** 1 h, **B)** 2 h, **C)** 3 h, **D)** 4 h, **E)** 5 h, **F)** 6 h, **G)** 14.5 h reaction. λ_{ex} = 440 nm, slit 2.0 nm. Obs: Spectra normalized with respect to maximum emission in NH_4OH 5 mol/L after 14.5 h of reaction.

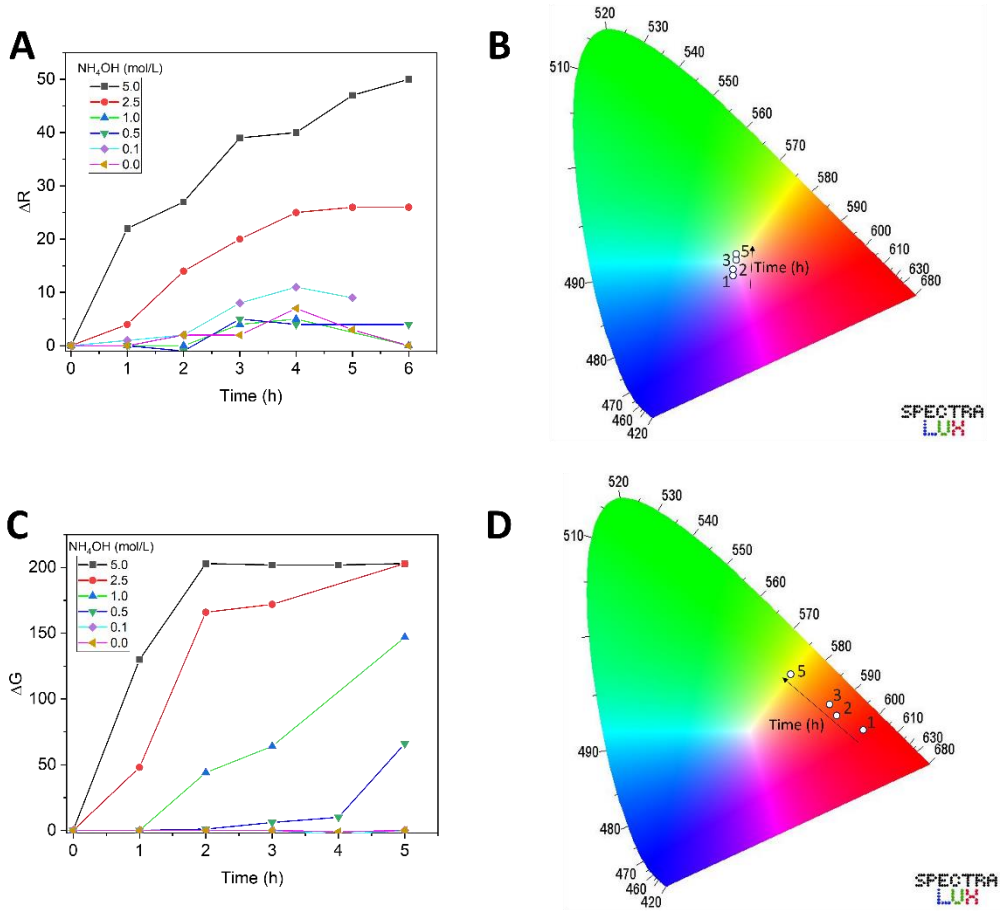

Fig. S12. **A)** ΔR values (extracted from **Fig. S10A** under visible light) vs time for the **BDP4@PMMA** after dipping in solutions containing different concentrations of NH_4OH (0 – 5 mol/L). **B)** CIE 1931 chromaticity diagram obtained through photography analysis from **Fig. S10A** (visible light) for **BDP4@PMMA** under 2.5 mol/L of NH_4OH over time (0 – 5 hours). **C)** ΔG values (extracted from **Fig. S10B** under UV light) vs time for the **BDP4@PMMA** after dipping in solutions containing different concentrations of NH_4OH (0 – 5 mol/L). **D)** CIE 1931 chromaticity diagram obtained through photography analysis from **Fig. S10B** (under UV light) for **BDP4@PMMA** under 1.0 mol/L of NH_4OH over time (0 – 5 hours).

3. Studies with BODIPY-doped Polymer particles

Table S2: Dynamic light scattering (DLS) data for BODIPY-doped polymer particles

Particles	Number [nm]	Volume [nm]	Intensity [nm]	Z-Average [nm]	PDI	ζ-potential [mV]
PMMA(µPs)control	164.2	220.2	220.2	221.3	0.099	-28.1
TPU(µPs)control	91.28	190.1	190.1	207.9	0.234	-25.9
BDP1(µPs)PMMA	141.8	255.0	255.0	247.6	0.154	-32.2
BDP1(µPs)TPU	105.7	190.1	190.1	182.6	0.167	-28.8
BDP2(µPs)PMMA	141.8	255.0	255.0	240.8	0.108	-30.4
BDP2(µPs)TPU	122.4	220.2	220.2	236.7	0.206	-26.5
BDP3(µPs)PMMA	122.4	220.2	220.2	228.0	0.156	-34.8
BDP3(µPs)TPU	105.7	190.1	190.1	194.2	0.165	-32.5
BDP4(µPs)PMMA	122.4	220.2	220.2	228.1	0.141	-30.3
BDP4(µPs)TPU	122.4	220.2	220.2	225.0	0.202	-35.5

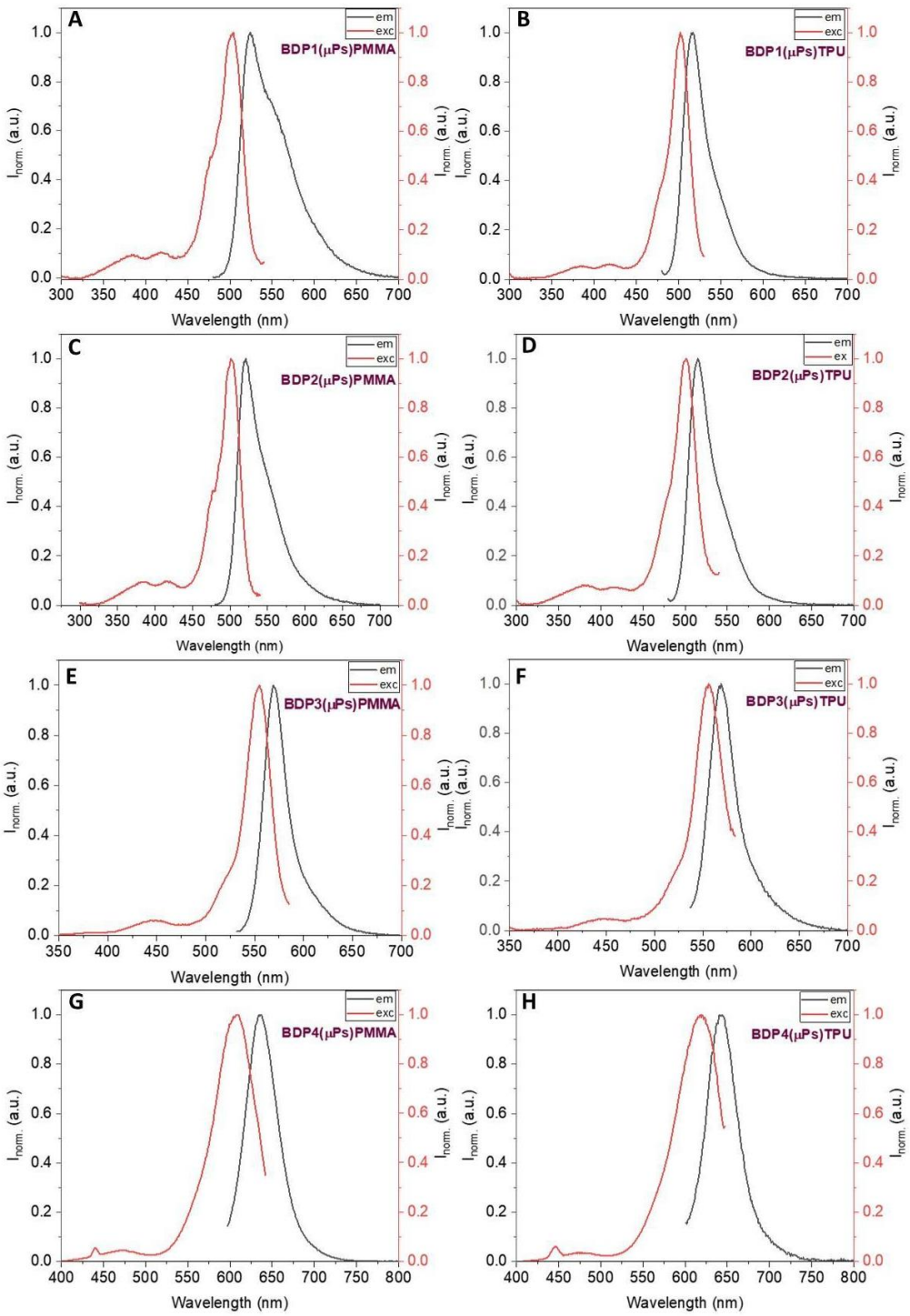

Fig. S13. Excitation and emission spectra of polymeric particles in water. Conditions: **BDP1(μPs)PMMA:** λ_{ex} = 470 nm, λ_{em} = 550 nm, slit 1.5 nm; **BDP1(μPs)TPU:** λ_{ex} = 470 nm, λ_{em} = 540 nm, slit 3.0 nm; **BDP2(μPs)PMMA:** λ_{ex} = 470 nm, λ_{em} = 550 nm, slit 1.5 nm; **BDP2(μPs)TPU**: λ_{ex} = 470 nm, λ_{em} = 540 nm, slit 3.0 nm; **BDP3(μPs)PMMA**: λ_{ex} = 520 nm, λ_{em} = 600 nm, slit 3.0 nm; **BDP3(μPs)TPU**: λ_{ex} = 520 nm, λ_{em} = 600 nm, slit 5.0 nm; **BDP4(μPs)PMMA**: λ_{ex} = 580 nm, λ_{em} = 660 nm, slit 5.0 nm; **BDP4(μPs)TPU**: λ_{ex} = 580 nm, λ_{em} = 670 nm, slit 5.0 nm

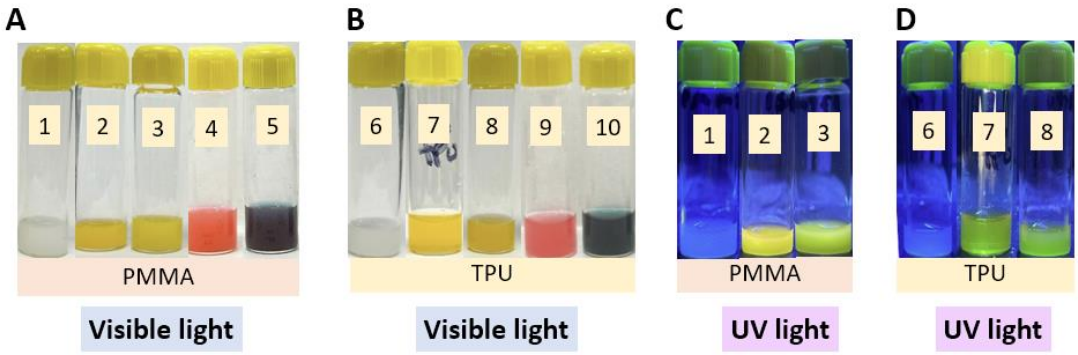

Fig. S14. Images of particle solutions under visible (**A, B**) and UV light (**C, D**) in water. Legend: **1** = PMMA(μPs)control, **2** = BDP1(μPs)PMMA, **3** = BDP2(μPs)PMMA, **4** = BDP3(μPs)PMMA, **5** = BDP4(μPs)PMMA, **6** = TPU(μPs)control, **7** = BDP1(μPs)TPU, **8** = BDP2(μPs)TPU, **9** = BDP3(μPs)TPU, **10** = BDP4(μPs)TPU.

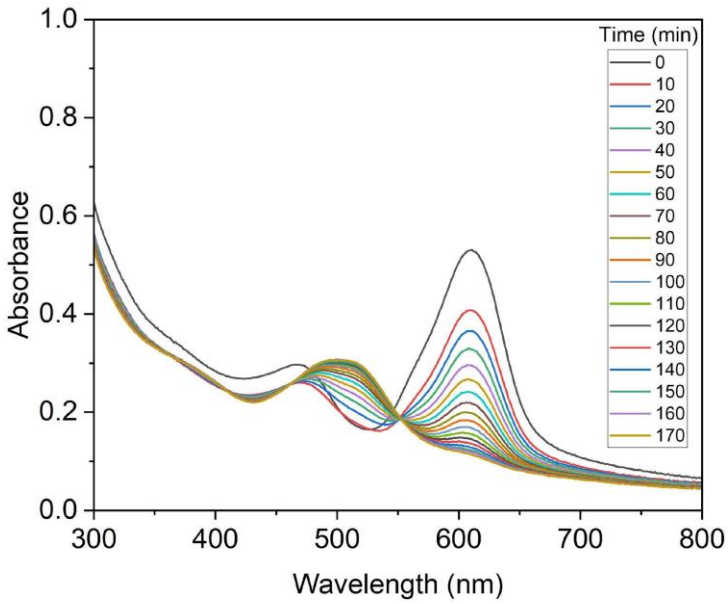

Fig. S15. Absorption spectra of **BDP4(μPs)TPU** particles in water upon addition of 0.59 mol/L of NH_4OH, recorded at 10 minute intervals.

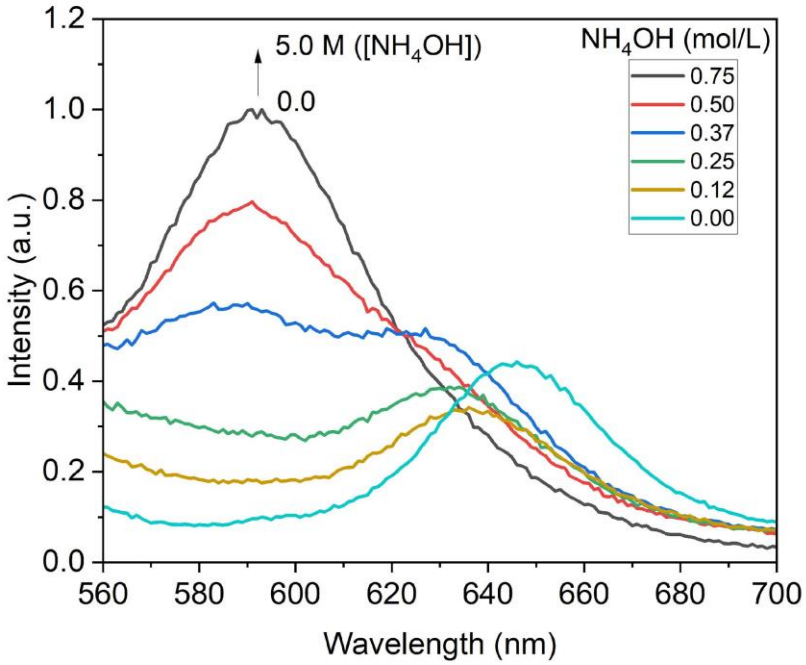

Fig. S16. Emission spectra of **BDP4(µPs)TPU particles** in water upon addition of different amounts of NH_4OH after 3 hours of reaction. λ_{ex} = 540 nm, slit 5.0 nm.

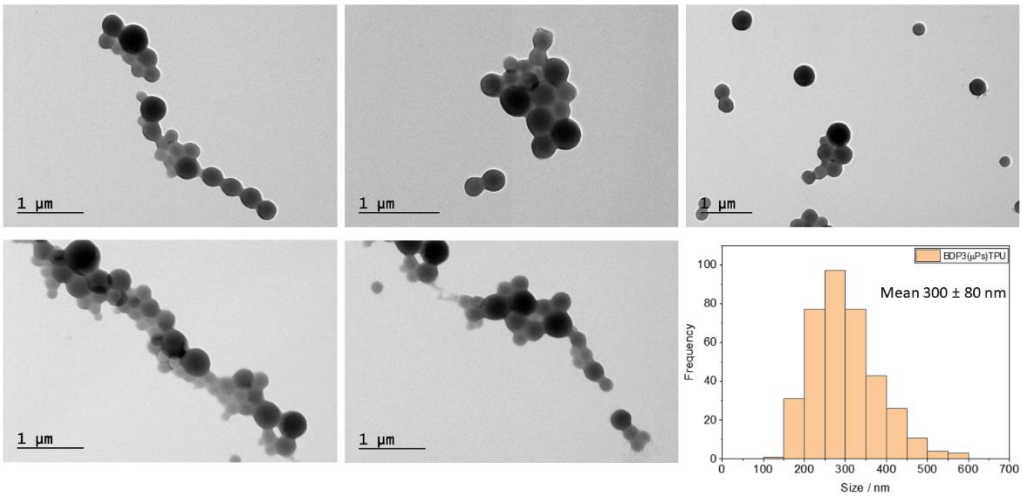

Fig. S17. Transmission Electron Microscopy (TEM) images for **BDP3(µPs)TPU** particles; bottom right: histogram of particle size distribution from TEM measurements for **BDP3(µPs)TPU.**

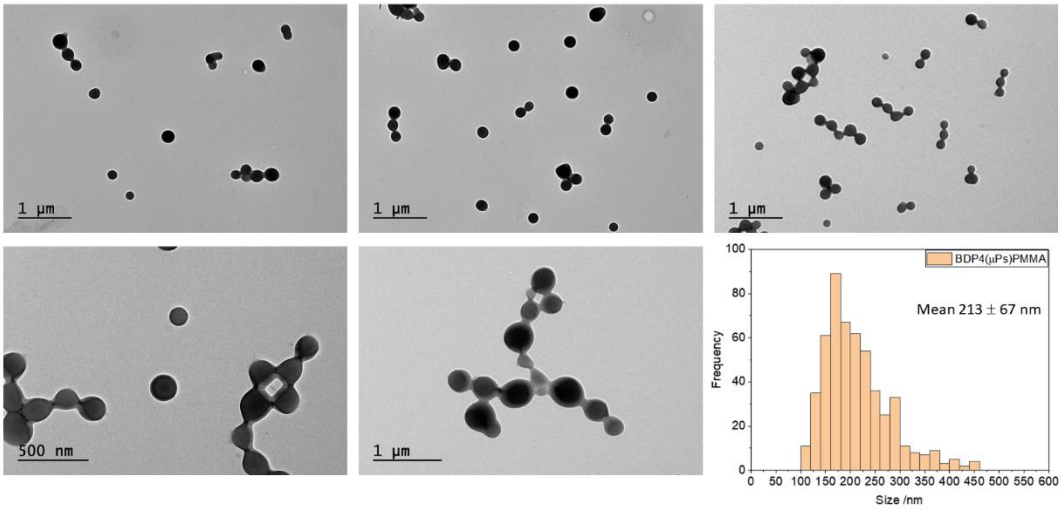

Fig. S18. Transmission Electron Microscopy (TEM) images for **BDP4(µPs)PMMA** particles; bottom right: histogram of particle size distribution from TEM measurements for **BDP4(µPs)PMMA.**

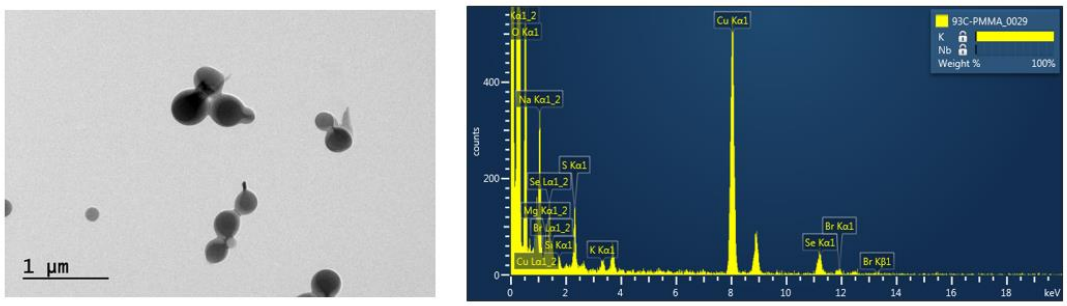

Fig. S19. Right: Transmission Electron Microscopy (TEM) image of **BDP4(µPs)PMMA** particles. Left: corresponding EDS spectra showing the chemical elements presents on the particles.

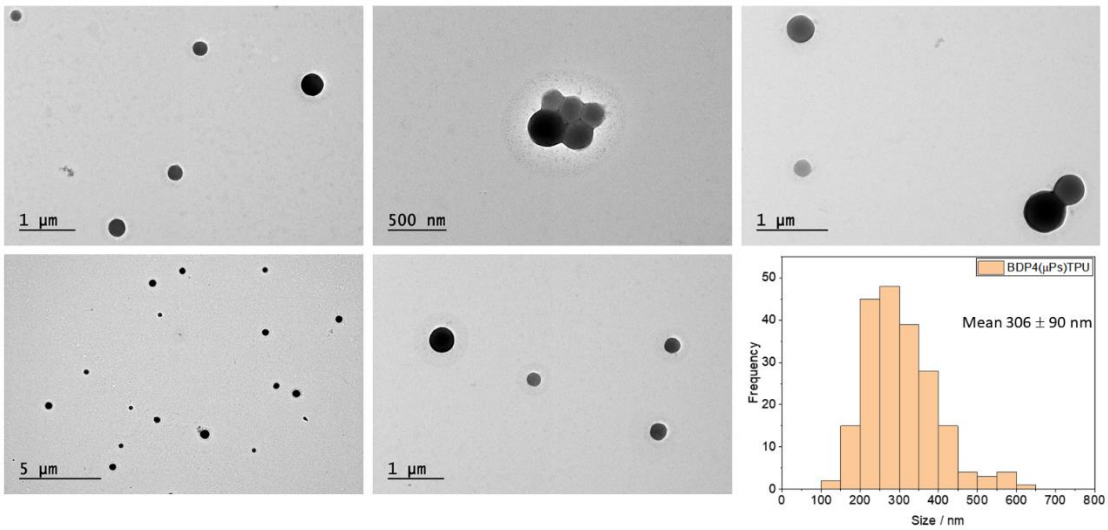

Fig. S20. Transmission Electron Microscopy (TEM) images of **BDP4(µPs)TPU** particles. Bottom right: histogram of particle size distribution from TEM measurements for **BDP4(µPs)TPU.**

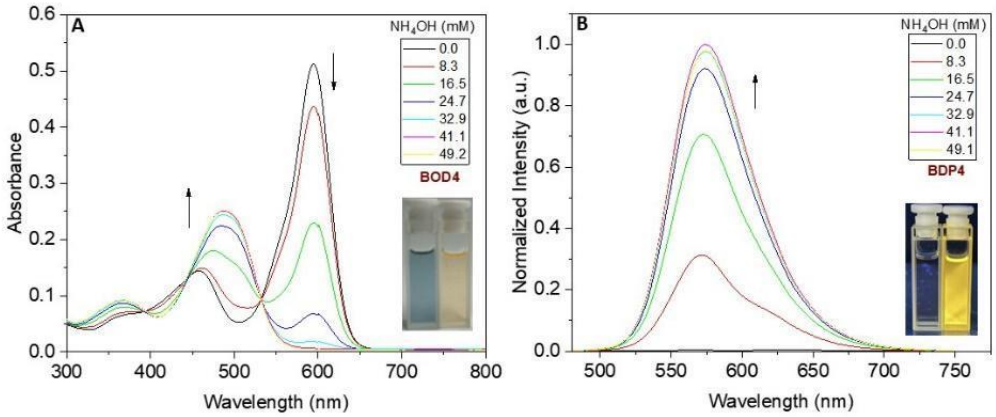

Fig. S21. Titration of **BDP4** with NH_4OH in THF. [BDP4] = 7.5 μmol/L. λ_{ex} = 470 nm, slit 2.5 nm

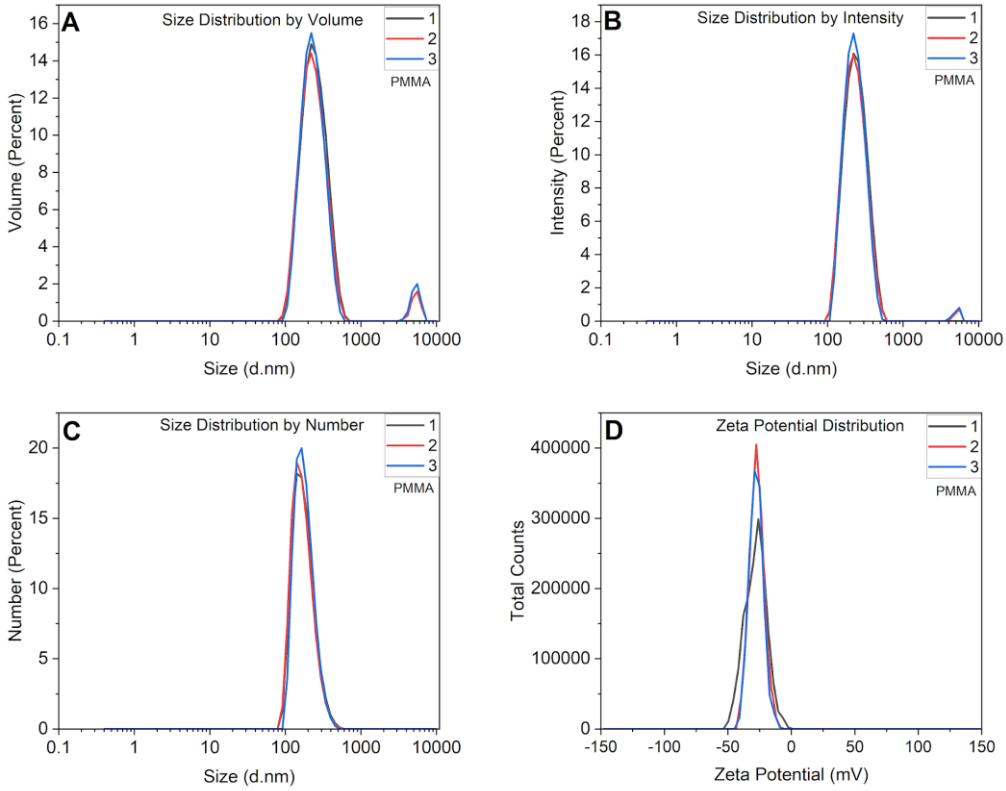

Fig. S22. Particle size distribution by **A)** volume, **B)** intensity, and **C)** number and **D)** zeta potential of **PMMA(μPs)control**.

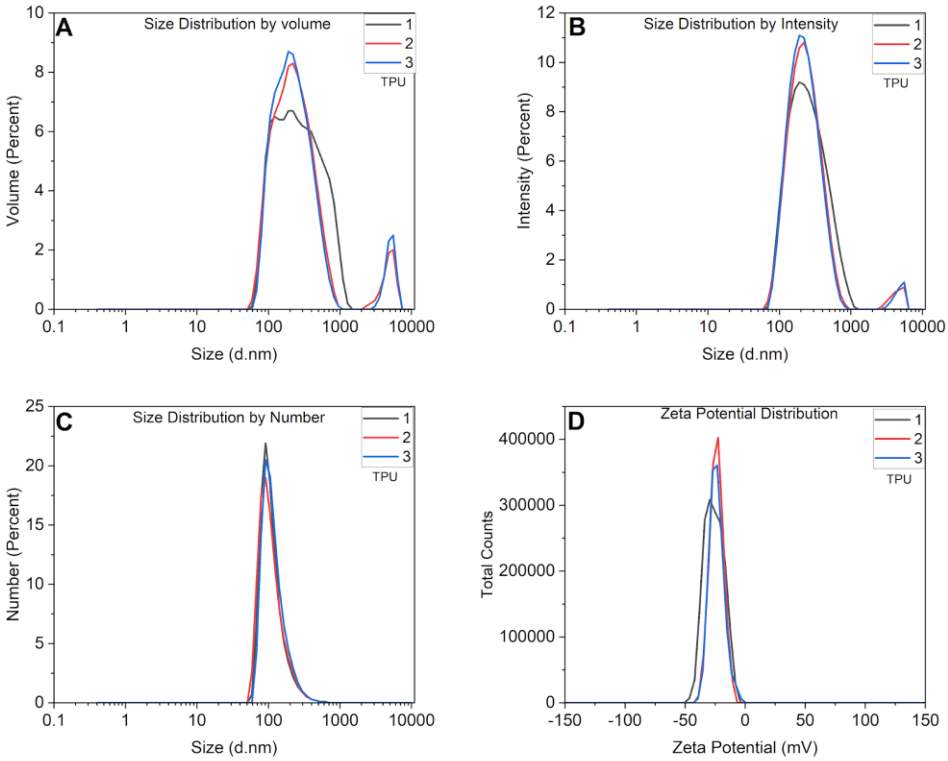

Fig. S23. Particle size distribution by **A)** volume, **B)** intensity, and **C)** number and **D)** zeta potential of **TPU(µPs)control**.

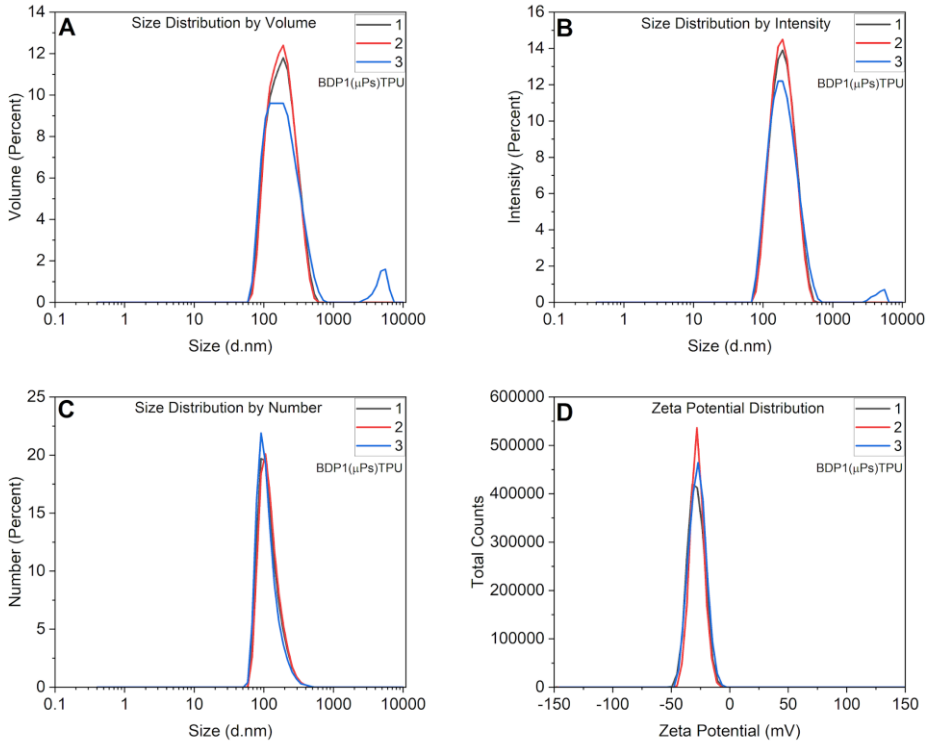

Fig. S24. Particle size distribution by **A)** volume, **B)** intensity, and **C)** number and **D)** zeta potential of **BDP1(µPs)TPU**.

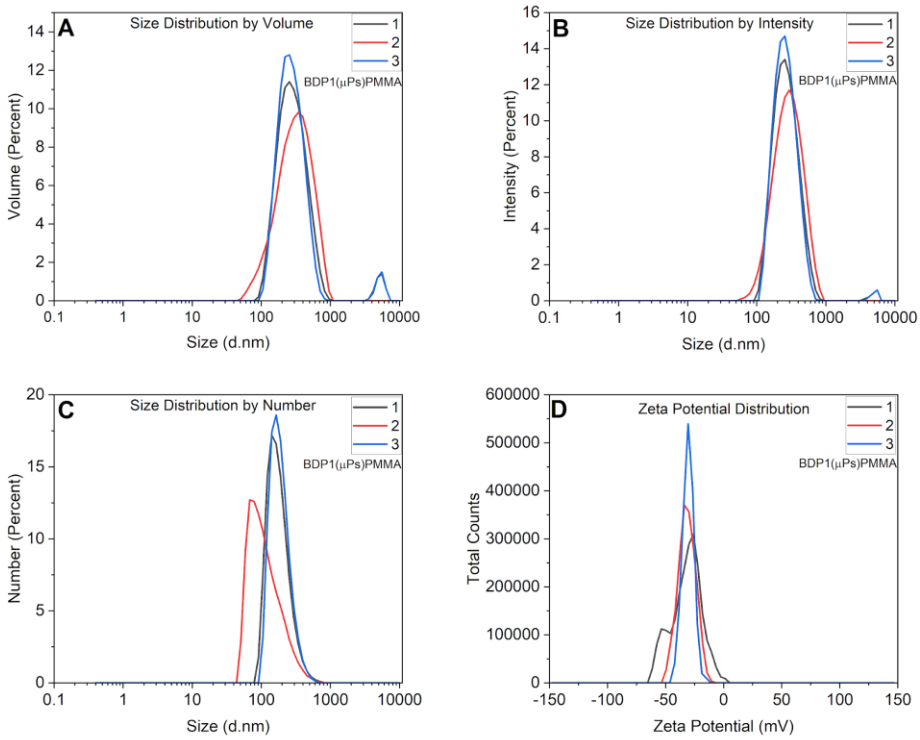

Fig. S25. Particle size distribution by **A)** volume, **B)** intensity, and **C)** number and **D)** zeta potential of **BDP1(μPs)PMMA**.

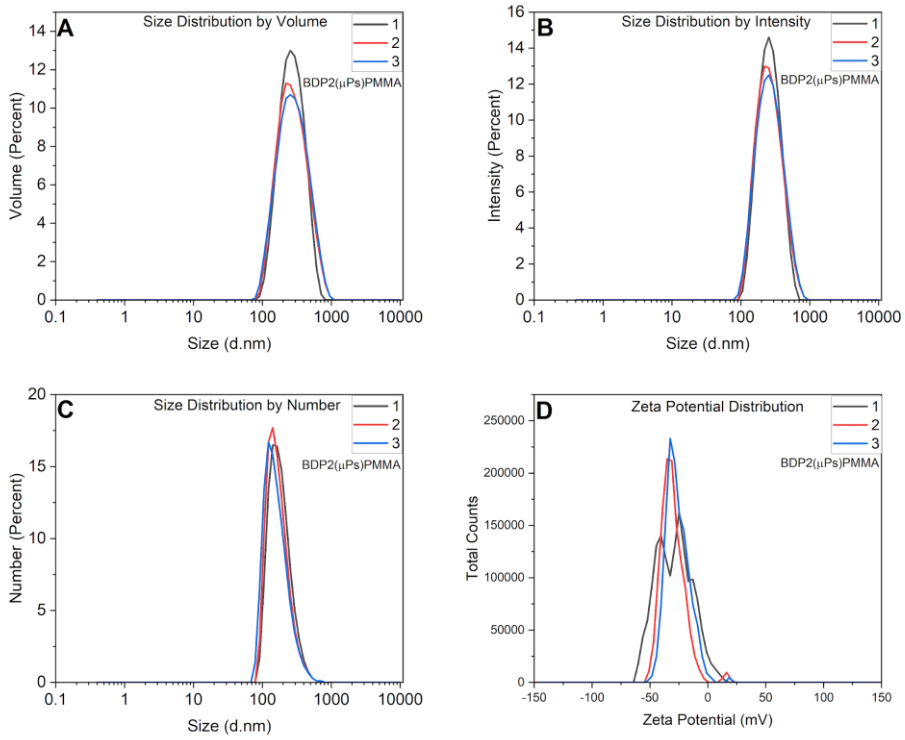

Fig. S26. Particle size distribution by **A)** volume, **B)** intensity, and **C)** number and **D)** zeta potential of **BDP2(μPs)PMMA**.

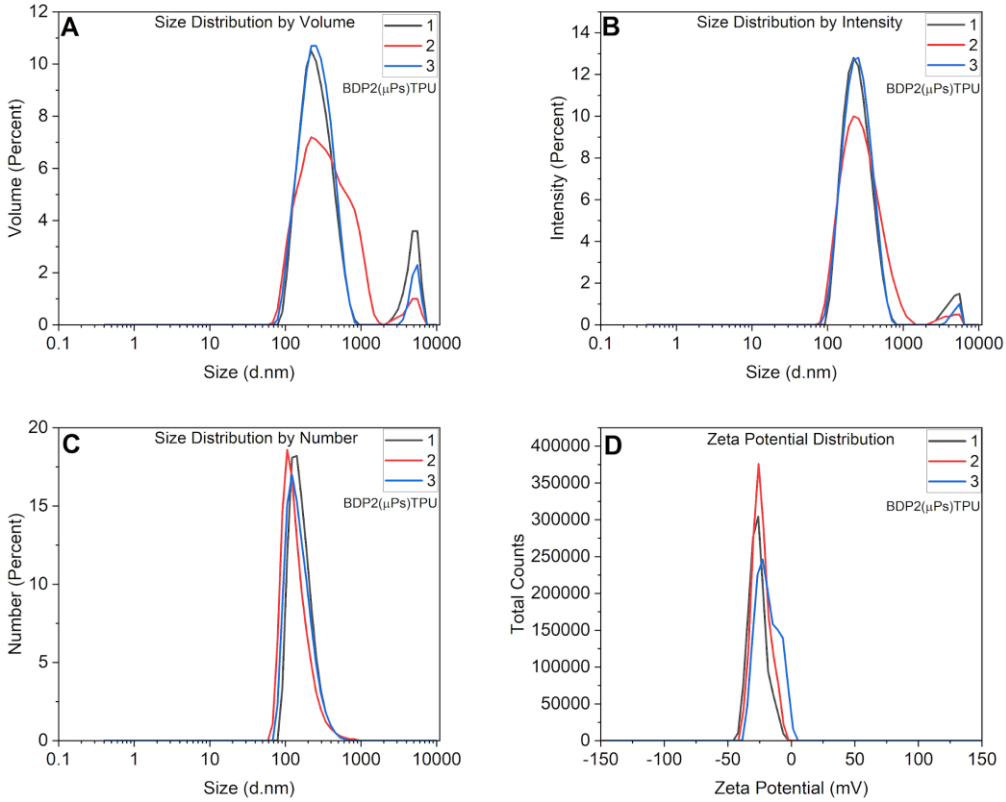

Fig. S27. Particle size distribution by **A)** volume, **B)** intensity, and **C)** number and **D)** zeta potential of **BDP2(µPs)TPU**.

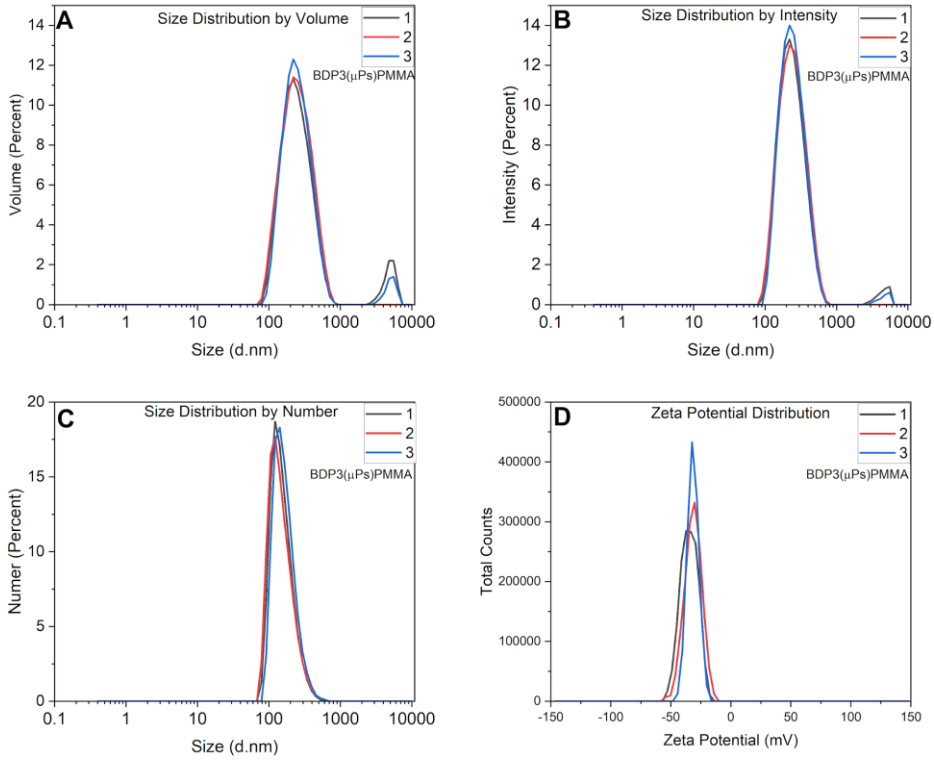

Fig. S28. Particle size distribution by **A)** volume, **B)** intensity, and **C)** number and **D)** zeta potential of **BDP3(µPs)PMMA.**

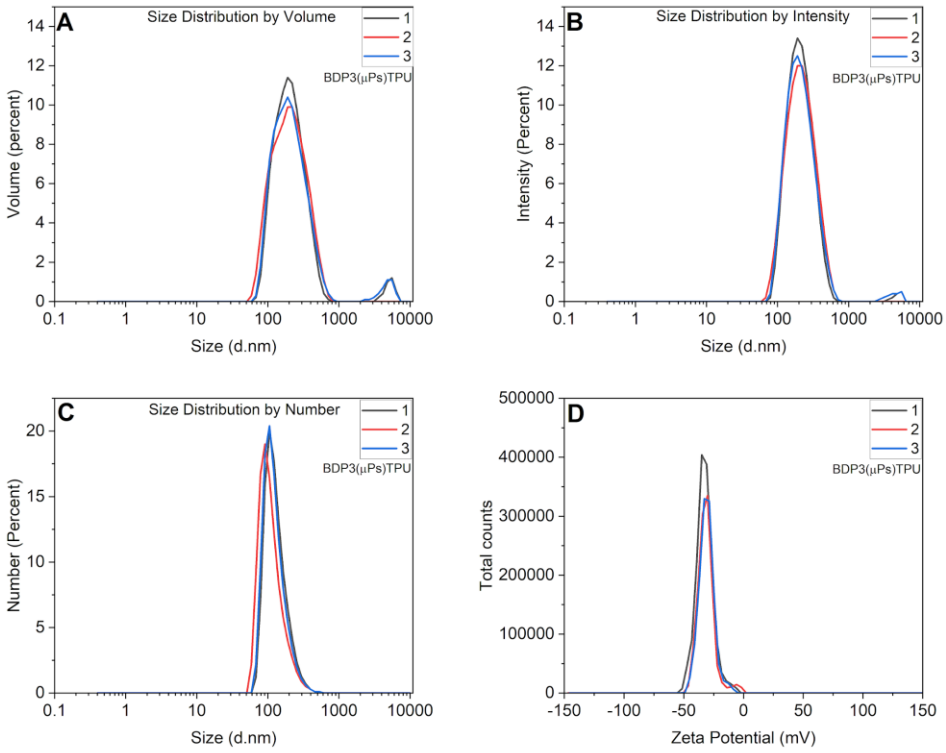

Fig. S29. Particle size distribution by **A)** volume, **B)** intensity, and **C)** number and **D)** zeta potential of **BDP3(μPs)TPU.**

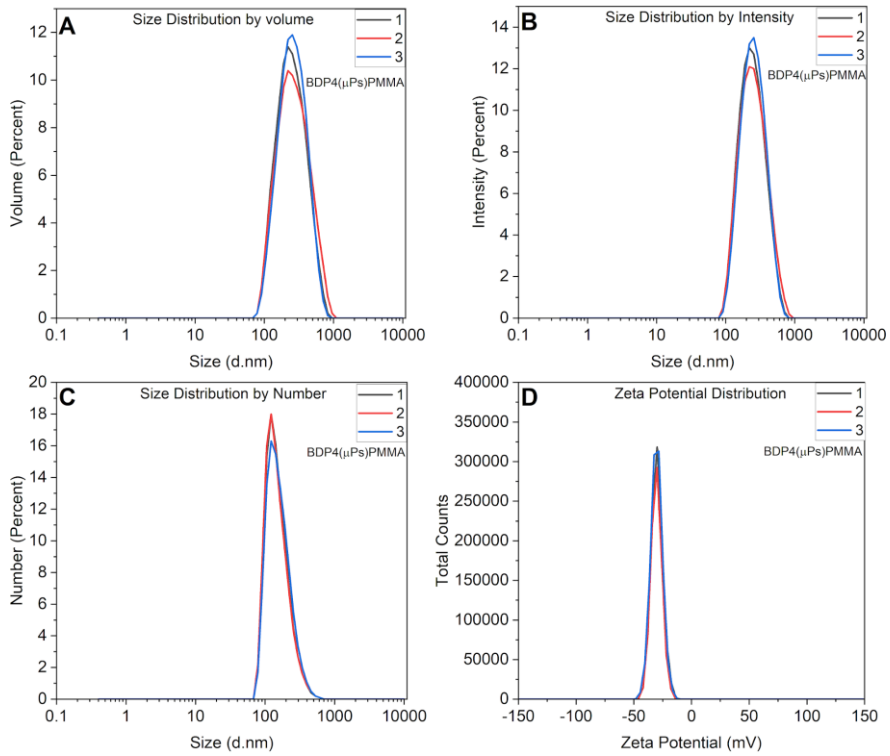

Fig. S30. Particle size distribution by **A)** volume, **B)** intensity, and **C)** number and **D)** zeta potential of **BDP4(μPs)PMMA.**

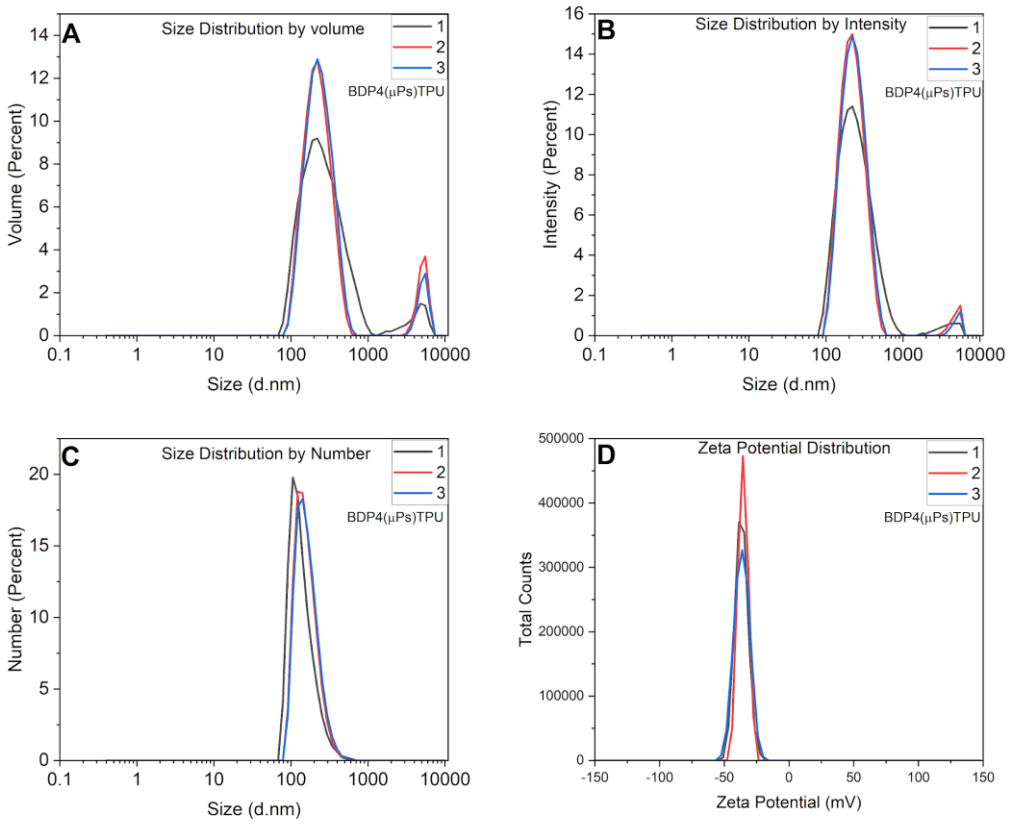

Fig. S31. Particle size distribution by **A)** volume, **B)** intensity, and **C)** number and **D)** zeta potential of **BDP4(μPs)TPU.**

4. Mass spectra analysis

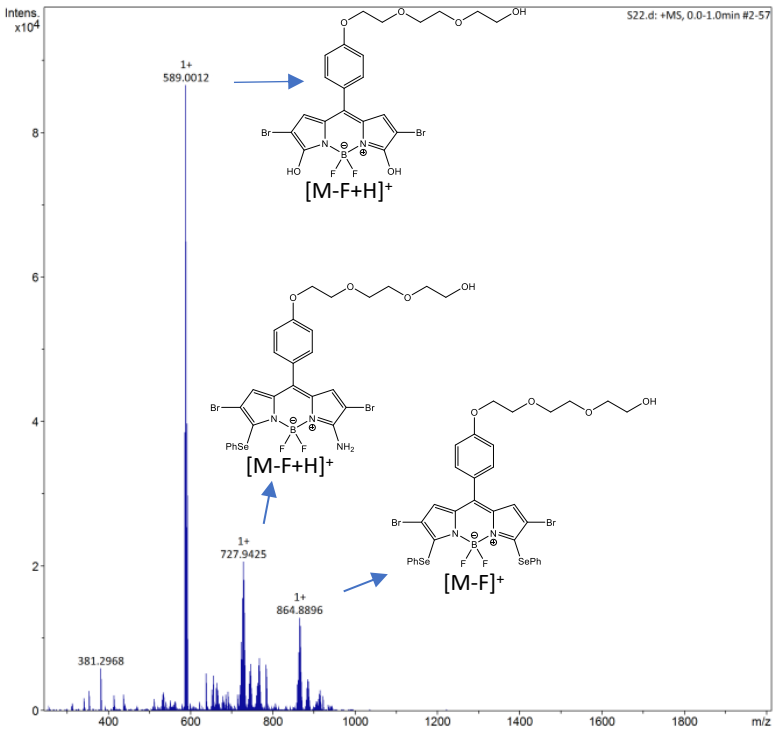

Fig. S32. HRMS spectra of **BDP4** after reaction with excess of NH_4OH. m/z $[M]^+$ for $C_{33}H_{29}BBr_2FN_2O_4Se_2$ = 864.8896. Calculated $[M]^+$ for $C_{33}H_{29}BBr_2FN_2O_4Se_2$ = 864.890085. m/z $[M+H]^+$ for $C_{27}H_{27}BBr_2FN_3O_4Se$ = 727.9425. Calculated $[M+H]^+$ for $C_{27}H_{27}BBr_2FN_3O_4Se$ = 727.967071. HRMS m/z $[M+H]^+$ for $C_{21}H_{22}BBr_2FN_2O_6$ = 589.0012. Calculated $[M+H]^+$ for $C_{21}H_{22}BBr_2FN_2O_6$ = 588.997930. HRMS m/z $[M+H]^+$ for $C_{27}H_{26}BBr_2F_2N_3O_4Se$ = 745.9548. Calculated $[M+H]^+$ for $C_{27}H_{26}BBr_2F_2N_3O_4Se$ = 745.957648.

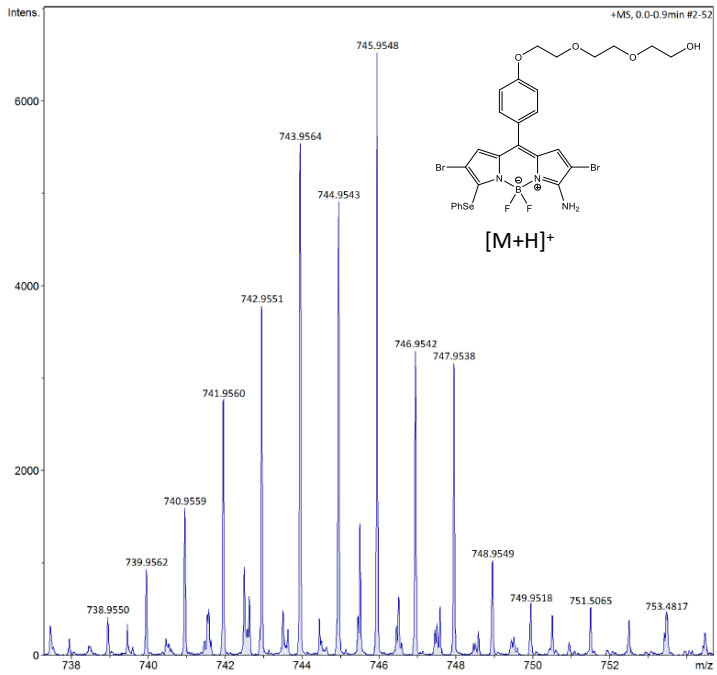

Fig. S33. HRMS for **BDP4-NH₂** m/z $[M+H]^+$ for $C_{27}H_{26}BBr_2F_2N_3O_4Se$ = 745.9548. Calculated $[M+H]^+$ for $C_{27}H_{26}BBr_2F_2N_3O_4Se$ = 745.957648.

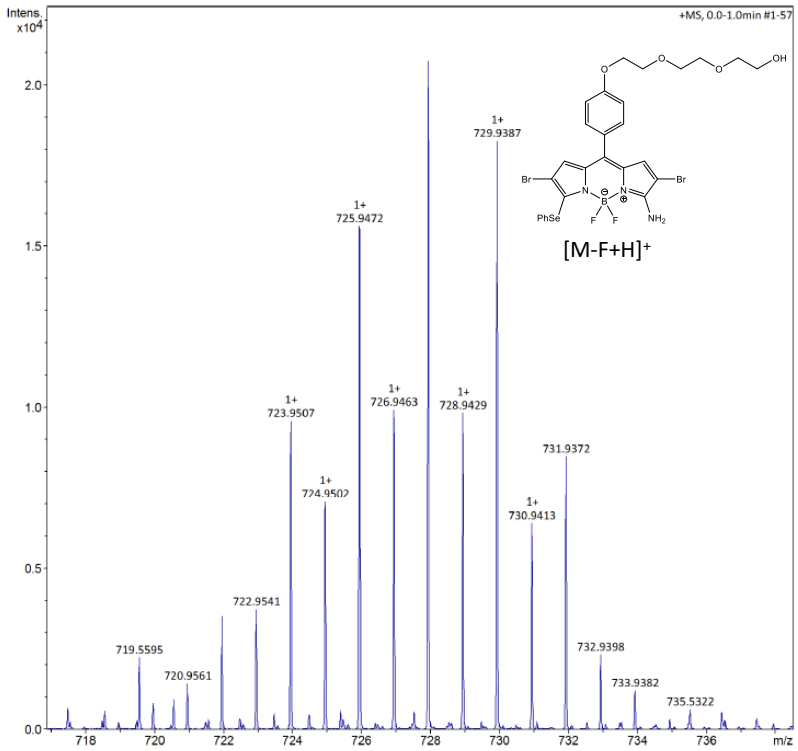

Fig. S34. HRMS for **BDP4-NH$_2$** m/z $[M+H]^+$ for $C_{27}H_{27}BBr_2FN_3O_4Se$ = 727.9425. Calculated $[M+H]^+$ for $C_{27}H_{27}BBr_2FN_3O_4Se$ = 727.967071.

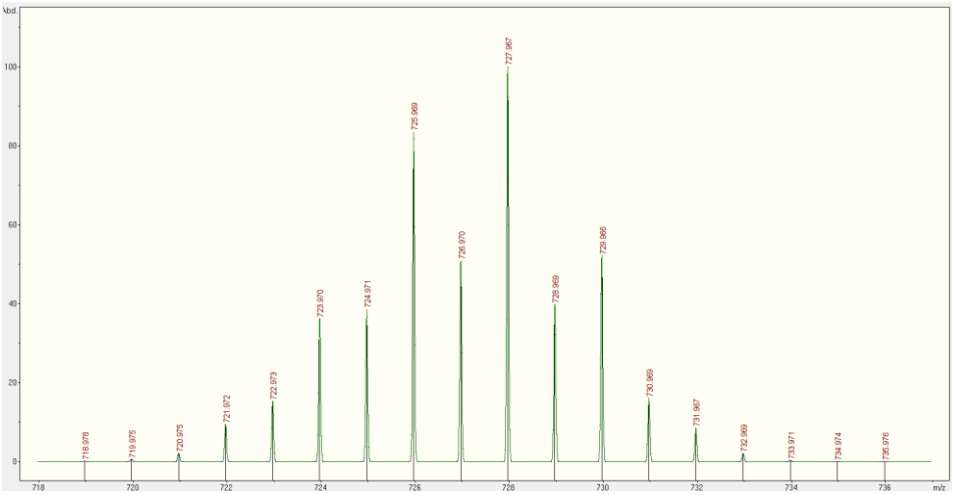

Fig. S35. Theoretical isotopic pattern for **BDP4-NH$_2$** obtained by software Compass IsotopePattern. HRMS (m/z) for $C_{27}H_{27}BBr_2FN_3O_4Se$: $[M+H]^+$ = 727.967071.

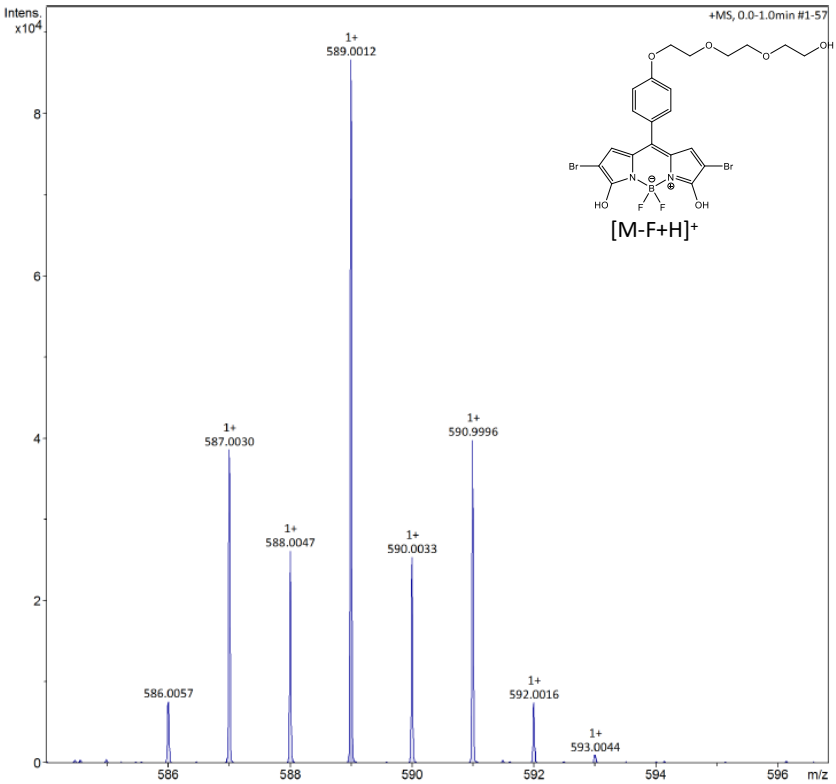

Fig. S36. HRMS for **BDP4-2OH** m/z $[M+H]^+$ for $C_{21}H_{22}BBr_2FN_2O_6$ = 589.0012. Calculated $[M+H]^+$ for $C_{21}H_{22}BBr_2FN_2O_6$ = 588.997930.

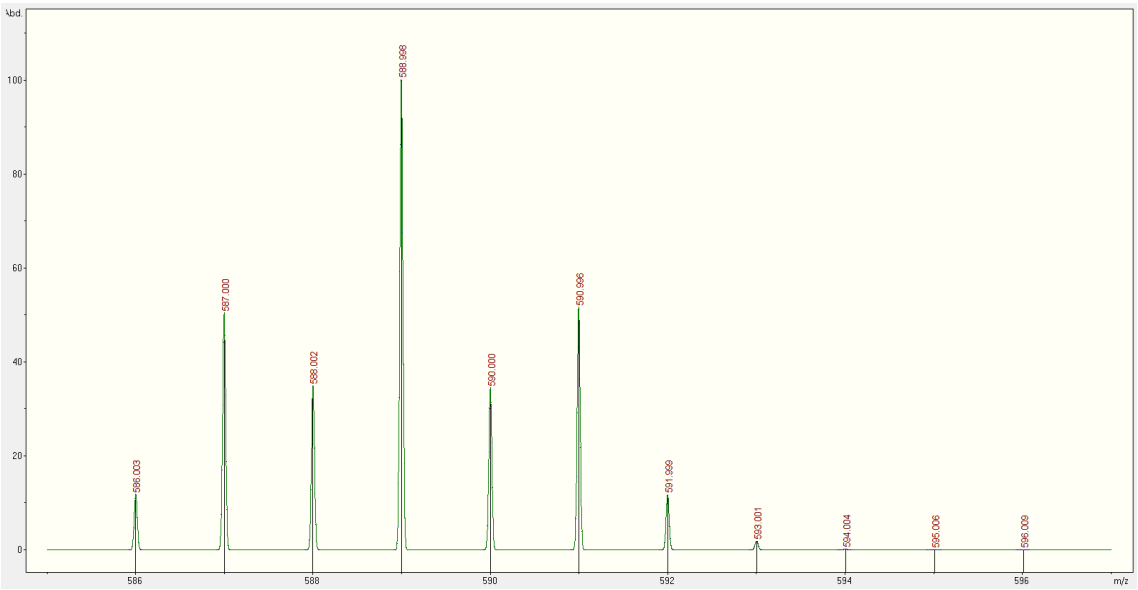

Fig. S37. Theoretical isotopic pattern for **BDP4-2OH** obtained by software Compass IsotopePattern. HRMS (m/z) for $C_{21}H_{22}BBr_2FN_2O_6$: $[M+H]^+$ = 588.997930.

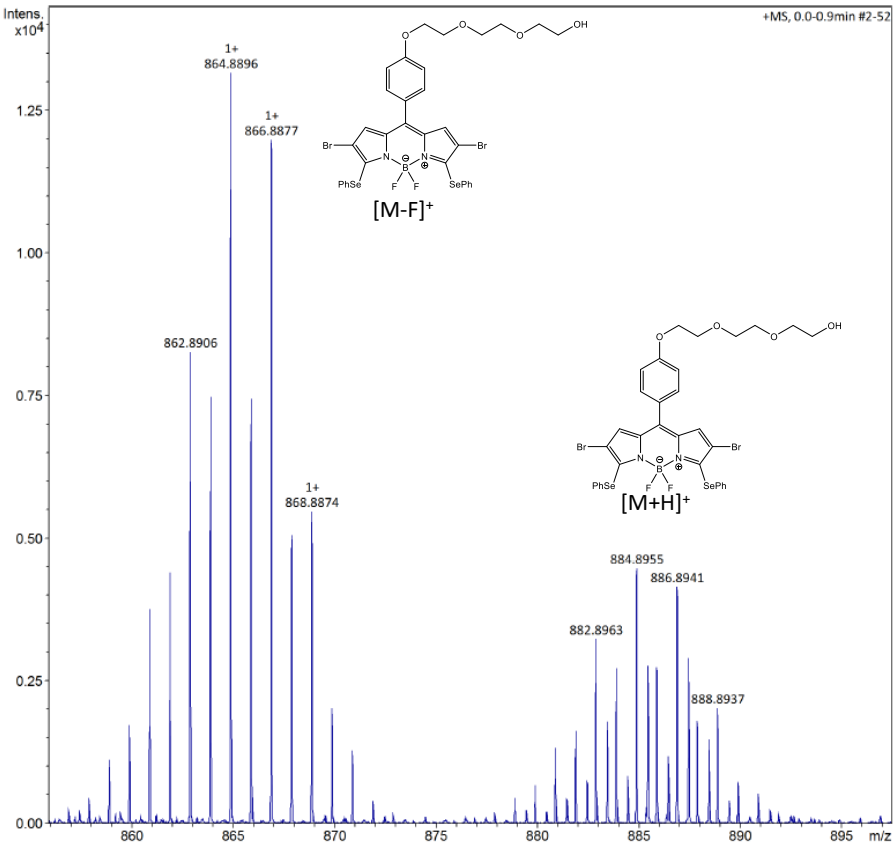

Fig. S38. HRMS for **BDP4** m/z $[M+H]^+$ for $C_{33}H_{29}BBr_2F_2N_2O_4Se_2$ = 884.8955. Calculated $[M+H]^+$ for $C_{33}H_{29}BBr_2F_2N_2O_4Se_2$ = 884.896314. HRMS for **BDP4** m/z $[M]^+$ for $C_{33}H_{29}BBr_2FN_2O_4Se_2$ = 864.8896. Calculated $[M]^+$ for $C_{33}H_{29}BBr_2FN_2O_4Se_2$ = 864.890085.

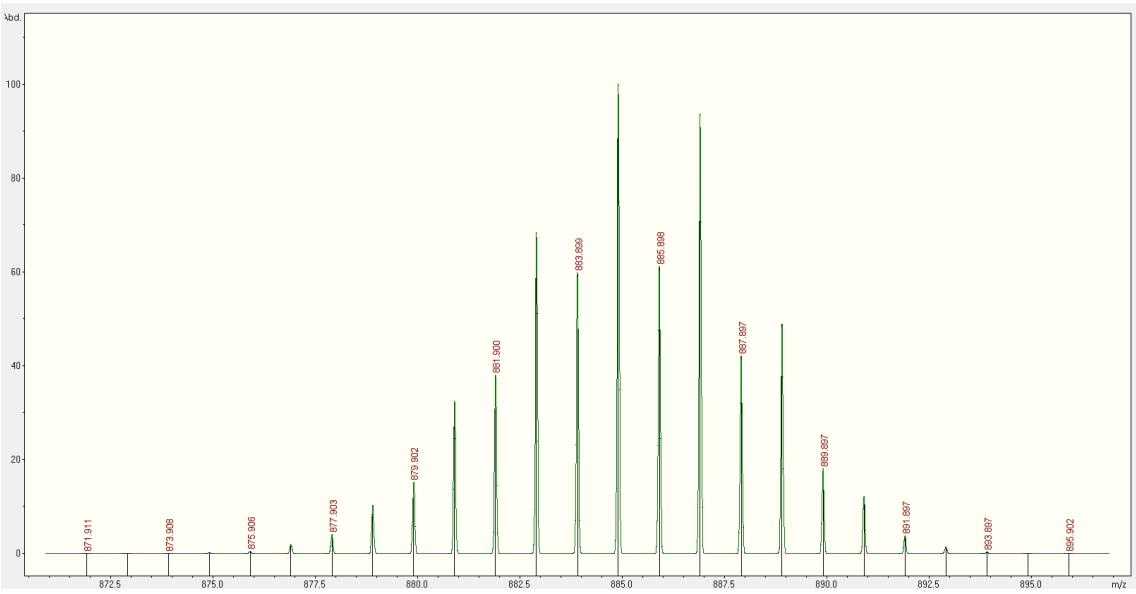

Fig. S39. Theoretical isotopic pattern for **BDP4** obtained by software Compass IsotopePattern. HRMS (m/z) for $C_{33}H_{29}BBr_2F_2N_2O_4Se_2$: $[M+H]^+$ =884.896314.